



UvA-DARE (Digital Academic Repository)

Seeing the forest for the fractions

Comparing soil organic matter fractionation methods using molecular features after forest stand conversion

Nikolaus, K.; Schellekens, J.; Mols, S.; Jansen, B.; Briones, M.J.I.; Desie, E.; Cornelis, J.T.; Absalah, S.; Muys, B.; Vancampenhout, K.

DOI

[10.1016/j.geoderma.2022.116280](https://doi.org/10.1016/j.geoderma.2022.116280)

Publication date

2023

Document Version

Final published version

Published in

Geoderma

License

CC BY

[Link to publication](#)

Citation for published version (APA):

Nikolaus, K., Schellekens, J., Mols, S., Jansen, B., Briones, M. J. I., Desie, E., Cornelis, J. T., Absalah, S., Muys, B., & Vancampenhout, K. (2023). Seeing the forest for the fractions: Comparing soil organic matter fractionation methods using molecular features after forest stand conversion. *Geoderma*, 430(116280), 430. Article 116280. <https://doi.org/10.1016/j.geoderma.2022.116280>

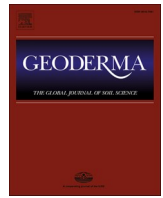
General rights

It is not permitted to download or to forward/distribute the text or part of it without the consent of the author(s) and/or copyright holder(s), other than for strictly personal, individual use, unless the work is under an open content license (like Creative Commons).

Disclaimer/Complaints regulations

If you believe that digital publication of certain material infringes any of your rights or (privacy) interests, please let the Library know, stating your reasons. In case of a legitimate complaint, the Library will make the material inaccessible and/or remove it from the website. Please Ask the Library: <https://uba.uva.nl/en/contact>, or a letter to: Library of the University of Amsterdam, Secretariat, P.O. Box 19185, 1000 GD Amsterdam, The Netherlands. You will be contacted as soon as possible.

UvA-DARE is a service provided by the library of the University of Amsterdam (<https://dare.uva.nl>)



Seeing the forest for the fractions – Comparing soil organic matter fractionation methods using molecular features after forest stand conversion

Karin Nikolaus^a, Judith Schellekens^{b,*}, Steven Mols^b, Boris Jansen^a, Maria J.I. Briones^c, Ellen Desie^b, Jean-Thomas Cornelis^d, Samira Absalah^a, Bart Muys^b, Karen Vancampenhout^b

^a University of Amsterdam, Institute for Biodiversity and Ecosystem Dynamics, P.O. Box 94240, NL1090GE Amsterdam, The Netherlands

^b Department of Earth and Environmental Sciences, KU Leuven Campus Geel, Kleinhofstraat 4, 2440 Geel, Belgium

^c Departamento de Ecología y Biología Animal, Universidad de Vigo, 36310 Vigo, Spain

^d University of British Columbia, Faculty of Land and Food Systems, V6T1Z4 Vancouver, Canada

ARTICLE INFO

Handling Editor: Cornelia Rumpel

Keywords:

Pyrolysis-GC/MS

Particulate organic matter (POM)

Water-extractable organic matter (WEOM)

Forest management

Soil carbon persistence

ABSTRACT

The molecular composition of soil organic matter (SOM) contains key information on the persistence of soil carbon (C) in relation to changes in vegetation and environmental factors. Depending on the ecosystem, analytical method and specific objectives, many SOM fractions and numerous fractionation schemes have been proposed to study soil C. However, the molecular composition and environmental significance of those different SOM fractions have not yet been compared systematically. We use a reverse fit approach to fill this knowledge gap: i.e. we chose a study area with a well-known land history to assess which information is stored in the most frequently analysed SOM fractions. The Gaume forest (Belgium) is an ancient deciduous forest (>200 years) in which small stands were converted to Norway spruce (*Picea abies*) 40–50 years ago. Those stands are located along a lithological gradient in soil buffering capacity. We investigated the molecular composition of bulk mineral soil samples and five organic SOM fractions by pyrolysis gas chromatography/mass spectrometry (Py-GC/MS). The SOM fractions included particulate OM (POM), water extractable OM (WEOM), and fractions obtained by alkaline extraction, including the traditionally used humic acid (HA) and fulvic acid (FA) and the total base extract from which they are obtained (BE). Our results indicate that pyrolysates of bulk mineral soil did not prove useful to reflect environmental changes after forest stand conversion. Principal Component Analysis indicated that within each organic fraction similar changes occurred when comparing soil depths, degree of SOM decomposition, litter inputs, and soil buffering capacity. However, only the HA and BE appeared successful in capturing all these processes: the degree of SOM decomposition was not expressed in pyrolysates from the POM, differences in litter input between forest stand types were not evidenced in the WEOM, and effects of buffering capacity were not demonstrated in the WEOM and FA fractions. Thus, the molecular composition of different SOM fractions can be used complementary to each other to study environmental and ecological effects of forest stand conversion on soil C dynamics.

1. Introduction

The composition of soil organic matter (SOM) at the molecular level can be used to understand key environmental processes (Man et al., 2022; Prescott and Vesterdal, 2021; Spaccini and Piccolo, 2020). However, the association of SOM with the mineral phase makes its structural analysis intricate. Soil minerals for instance interfere with solid state nuclear magnetic resonance (NMR) measurements due to paramagnetic

properties, they can mask molecular information in infrared spectra, and can act as catalyst in thermally assisted methods (Kögel-Knabner, 2000). SOM purification or isolation is therefore a common practice prior to structural analysis of SOM.

SOM has traditionally been separated into a few operationally defined fractions, i.e., humic acid (HA), fulvic acid (FA) and humin (Stevenson, 1982). These so called ‘humic substances’ formed the foundation of SOM research for the last two centuries and they continue

* Corresponding author.

E-mail address: schellekens.j@hetnet.nl (J. Schellekens).

<https://doi.org/10.1016/j.geoderma.2022.116280>

Received 5 July 2022; Received in revised form 17 October 2022; Accepted 18 November 2022

Available online 6 December 2022

0016-7061/© 2022 The Authors. Published by Elsevier B.V. This is an open access article under the CC BY license (<http://creativecommons.org/licenses/by/4.0/>).

to be successfully used in some disciplines (Olk et al., 2019). However, their functional and ecological relevance is currently being questioned, because HA and FA are obtained under alkaline conditions that do not normally occur in nature (Kleber and Lehmann, 2019). Consequently, chemical methods to isolate SOM have been increasingly replaced by physical procedures, including particulate organic matter (POM) and several size-classes of mineral-associated organic matter (Lavallee et al., 2020). Although the distribution of C among these mineral fractions has been shown to provide valuable information on functional SOM pools in terms of soil C persistence (e.g. Zimmermann et al., 2007), it does not solve the constraints associated to the analysis of non-targeted SOM as the mineral-associated organic matter remains bound to bivalent and trivalent cations and clay-sized minerals.

There is an overwhelming body of literature that shows that structural information at the molecular level can provide insights in ecological (soil) processes and their environmental controls, for both alkaline extraction and pool-based SOM isolation methods (Carrington et al., 2012; Filep et al., 2022; Man et al., 2022; Nierop et al., 2001; Roscoe and Buurman, 2003; Savarese et al., 2021). Yet work that compares structural information among SOM fractions obtained with both types of SOM isolation methods in a field context remains scarce (Barreto et al., 2021; Buurman and Roscoe, 2011; Chiapini et al., 2018; Han et al., 2021; Justi et al., 2017; Nierop and Buurman, 1998).

We use a reverse fit approach to contribute to this knowledge gap: i. e. we chose a study area with a well-known land history to assess which environmental information is reflected in several frequently analysed SOM fractions. The chosen SOM fractions included two pool-based fractions (POM and water-extractable organic matter (WEOM)), three SOM fractions obtained with alkaline extraction (the traditional HA and FA, and the total base extract of which they are obtained (BE)), and bulk mineral soil (Bulk). To obtain structural information at the molecular level we analysed these SOM fractions with pyrolysis gas chromatography/mass spectrometry (Py-GC/MS). Molecules identified by Py-GC/MS can be linked to specific plant and microbial origins (biomarkers) and to the degree of SOM decomposition (Buurman et al., 2007; Carr et al., 2010; Kaal et al., 2017; Nierop et al., 2001; Tinoco et al., 2002).

We systematically compared Py-GC/MS results obtained from the SOM fractions for a well-characterised forest site in terms of soil processes, i.e., the Gaume forest in Belgium (Brock et al., 2019; Desie et al., 2021, 2019; Verstraeten et al., 2018). In this ancient deciduous forest, small stands of Norway spruce (*Picea abies*) were planted 40–50 years ago. A twin-plot design of paired deciduous and coniferous plots has been laid out there to evaluate the effects of overstorey conversion on different compartments of the ecosystem, including geochemical properties, earthworm communities, microbial catabolic diversity, and soil C stocks (Brock et al., 2019; Desie et al., 2021, 2019; Verstraeten et al., 2018). The twin-plot design also allows tracing of the input material because gymnosperms and angiosperms differ in their lignin composition (Hedges and Mann, 1979). Finally, the Gaume forest spans a lithological gradient of Jurassic parent materials, resulting in a different buffering capacity of its soils. The twin-plots were selected along this lithological gradient. The site is thus ideal to examine whether, and to which extent, soil legacies caused by stand conversion can be detected in the molecular composition of different SOM fractions.

2. Materials and methods

2.1. Study site and soil sampling

The Gaume forest is a large deciduous forest in the Virton district in southern Belgium (49°37'N, 5°33'E), which has been continuously forested since records started in 1775. Dominant tree species include Pedunculate oak (*Quercus robur*), Beech (*Fagus sylvatica*) and European hornbeam (*Carpinus betulus*). Within this forest, Norway spruce (*Picea abies*) was planted in patches (2–15 ha) 40–50 years ago (Fig. S1, Table S1). The area has an elevation between 250 and 360 m a.s.l., with

an annual mean temperature of 8.7 °C and annual precipitation is 873 mm, respectively. Soils have evolved from two Jurassic formations (Arlon and Luxembourg), consisting of deposits of calcareous sandstones with a varying marl content. Differences in parent material have led to the development of different soil types, i.e., Luvisols, Alisols, and Cambisols (IUSS Working Group WRB, 2015) with varying soil acid buffering properties. For a detailed description of the site please refer to Verstraeten et al. (2018). Based on the differences in soil acid buffering properties prior to conversion (including pH, cation exchange capacity, and base saturation) two contrasting soil process domains (*sensu* Vitousek and Chadwick, 2013) were defined, i.e. the base-dominated soil process domain (further named 'Exchange Domain') and the aluminium-dominated soil process domain (further 'Aluminium Domain'). Below the threshold (pH-H₂O of ca. 4.5 and base saturation of 30 %), i.e. in the Aluminium Domain, critical changes occur in solubility of metals and organic compounds, in organo-mineral interactions, in soil faunal- and microbial communities, and in soil C dynamics (Desie et al., 2021).

The experimental set up consisted of 6 twin-plots (deciduous and spruce), from which the deciduous plots represented both soil process domains (plots 8, 12, 17, 21, 25 and 36, Table S1), while all stands shifted to the Aluminium Domain after conversion to spruce (Desie et al., 2019). Twin plots consist of two neighbouring stands (native deciduous and planted spruce) separated <60 m apart, hence assuring that soil, elevation, and slope are comparable (Desie et al., 2019). Because bark-beetle infestations seriously affected the spruce stands since 2020, archived soil samples collected by Desie et al. (2019) were used for this study (Table S2). Soil samples were taken with a soil corer. Each soil sample was a composite of five sub-samples taken from a plot of 10 × 10 m. From each plot two soil depths were used (topsoil: 0–5 cm and subsoil: 25–30 cm), resulting in a total number of 24 samples for SOM fractionation (i.e., 6 plots, 2 stands, 2 depths).

2.2. SOM fractionation

A schematic overview of the SOM fractionation procedure is given in Fig. 1. All soil samples were sieved (<2 mm) prior to further treatment.

Subsamples (1 g) from the sieved soil were ground and homogenised for analysis. This bulk mineral soil is further referred to as 'Bulk'.

To obtain POM, aggregates of the sieved soil samples were dispersed using an ultrasonic probe (3.5 min, energy output: 22 J ml⁻¹). Subsequently, the samples were wet sieved (<63 µm) for 2 min followed by a density separation using sodium polytungstate (density: 1.8 g cm⁻³; Desie et al., 2019).

For the WEOM extraction, the sieved soil was shaken (150 rpm for 48 h) with distilled water (1/10 m/v) and centrifuged (3000 rpm for 20 min). The supernatant was filtered (0.7 µm glass fibre filters; VWR) following Denis et al. (2017). The filtered solution was freeze-dried and homogenised.

To obtain the BE fraction, NaOH (0.1 M) was added to the sieved soil (1/10 w/v), shaken (120 rpm) overnight, centrifuged (3000 rpm for 30 min), and the supernatant separated from the residue. This procedure was repeated once for the subsoil and twice for the topsoil as the latter samples contained more SOM (Table 1). The supernatants were filtered through glass fibre filters (0.7 µm; VWR) and a subsample was separated to represent the total BE. The remaining volume of the supernatant was used for separation into HA and FA. To this end, HCl (6 M) was added until pH 1–2 was reached to separate FA (supernatant) and HA (precipitate) (Sparks et al., 1996). The BE was acidified with HCl to pH 1–2, and thereafter 1 ml concentrated HF (48 %) was added to all three fractions to demineralize the sample (Nierop and Buurman, 1998). To remove excess salts, the solutions were dialysed (6–8 kD; Preston et al., 1994) freeze-dried and homogenised.

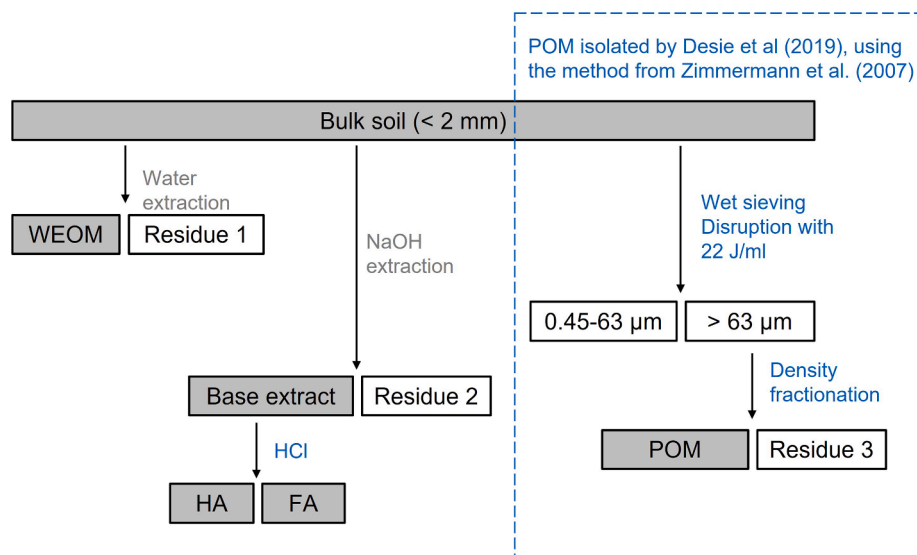


Fig. 1. SOM fractionation scheme. The coloured cells reflect SOM fractions that were analysed by Py-GC/MS.

Table 1

Medians of sample characteristics for different sample classes. The bold numbers indicate significant differences between the classes. Significance was tested by means of the Kruskal-Wallis test. Because most characteristics showed a significant difference for soil depth, the medians for forest stand type, soil process domain, and geological formation are additionally given separately for top- and subsoil in Table S3.

		C_{bulk} (%)	$C_{\text{POM}}^{\text{a}}$ (% of C)	C_{BE} (% of C)	C_{WEOM} (mg/l)	$\delta^{13}\text{C}_{\text{WEOM}}$ (‰)	$\text{C}/\text{N}_{\text{bulk}}$
Soil depth	Subsoil	0.7	22.8	53.4	20.8	-24.2	11.2
	Topsoil	3.5	24.2	45.3	104.7	-26.2	20.3
Forest stand type	Deciduous	1.5	22.5	47.2	41.6	-25.3	12.5
	Spruce	2.1	23.8	53.4	56.7	-25.8	17.6
Soil process domain ^b	Aluminium	1.5	23.5	52.1	39.2	-25.8	16.9
	Exchange	1.7	23.5	49.3	50.3	-24.8	12.1
Geological formation	Arlon	1.7	23.6	53.3	50.3	-25.0	12.1
	Luxembourg	1.5	23.3	50.3	39.6	-25.4	15.2

^a Data from Desie et al. (2019).

^b The soil process domain refers to the plot before forest conversion, after conversion to spruce all plots belonged to the Aluminium Domain.

2.3. Py-GC/MS

The Bulk, POM and WEOM samples were analysed for all six plots (plots 8, 12, 17, 21, 25 and 36), whereas in the case of the BE and the HA and FA fractions only sufficient material was available for four plots (plots 12, 21, 25 and 36). This resulted in a total number of 120 samples to analyse the molecular composition with Py-GC/MS. To facilitate comparison of our approach with previous studies on the same site, methodologies are summarized in Table S2.

Py-GC/MS analyses were carried out at the IBED laboratory (University of Amsterdam). A multi-shot furnace pyrolyser (EGA/Py-3030D; Frontier Lab, Japan) with an AS-1020E auto-sampler was used, coupled to a Thermo Scientific Trace 1300 gas chromatograph (GC; Milan, Italy) with a Rx1-1 ms fused silica column (Restek: 30 m; 0.25 mm i.d.). The column was coated with di-methyl poly-siloxane (film thickness: 0.50 μm) and the carrier gas was helium (constant flow: 1 ml/min). The pyrolyser was set to 600 °C (0.8 min) and the interface temperature between pyrolyser and GC was set to 300 °C. The injection temperature to the GC (operated in 100:1 split mode) was 250 °C. The GC was started at 40 °C (hold time: 1 min, heating rate: 7.0 °C/min) and the final temperature was 320 °C (hold time: 10 min). A Thermo Scientific ISQ 7000 Single Quadrupole MS (Milan, Italy) (mass to charge ratio (m/z): 47–500; ionization energy: 70 eV) was coupled to the GC (Brock et al.,

2020; Justi et al., 2017). Because an auto-sampler was used, the amount of sample material was determined upon calibration with pilot samples. Depending on sample type, i.e., organic samples (SOM fractions) or mineral soil (Bulk), different sample amounts were used. For the SOM fractions 100 μg yielded sufficient peak intensities. For the Bulk the amount was increased up to 300 μg . Beyond that quantity a higher input did not yield a substantially higher peak intensity.

The identification of pyrolysis products was performed in Masslab and using the NIST 2014 library. In total, 64 pyrolysis products were selected for quantification, including at least the 20 largest peaks for each sample. Some non-dominant lignin products were also included because they provide key information about the origin of SOM inputs (i.e., deciduous vs coniferous species; Hedges and Mann, 1979; Thevenot et al., 2010). Selected products were classified according to their chemical nature into seven groups: benzenes, benzofurans, carbohydrates, phenols, lignin products, N-containing compounds, and polycyclic aromatic hydrocarbons (PAHs) (Appendix A). Aliphatic products obtained with thermally assisted hydrolysis and methylation in the presence of tetramethylammonium hydroxide (THM-TMAH) can provide information about plant biopolymers (Nierop and Buurman, 1998) and were used as such in soil samples from the Gaume forest by Brock et al. (2019). However, given their very low abundance in the pyrolysates of most samples, in combination with the difficulty in interpreting

aliphatics from Py-GC/MS results (Schellekens and Buurman, 2011), the aliphatic group was excluded from this study.

To quantify each selected pyrolysis product, the two characteristic ion fragments of the targeted product were used (Appendix A; Buurman et al., 2007). This yields a partial pyrogram and the area of the targeted peak is calculated by integration. For each sample, the sum of all quantified peak areas is set to 100 %. The relative abundance of a pyrolysis product in a sample was calculated as percentage of this sum. Abundances of pyrolysis products are therefore semi-quantitative.

2.4. Total organic C and N

To compare the qualitative interpretation of the pyrolysis products with quantitative measurements, the distribution of C among the SOM fractions, and total C and N contents of bulk soil samples were measured. The C and N content of the bulk soil was measured by dry combustion (Vario EL cube, Elementar GmbH). To calculate the proportion of C in the BE relative to the bulk soil, the C content of the residue after alkaline extraction was determined using the same method. The contribution of the BE to the total SOM (C_{BE}) was obtained as the difference between the bulk soil and the residue (Residue-2 in Fig. 1). The C content of the POM fraction was determined earlier by Desie et al. (2019).

For the soluble fractions (WEOM, BE, and FA) the C content was measured as dissolved organic carbon (DOC). The DOC content of BE and FA samples was measured in three replicates by combustion, using a vario TOC cube (Elementar GmbH). The DOC content of WEOM samples were analysed using a wet oxidation TOC analyser (IO Analytical Aurora 1030 W) coupled with an isotope ratio mass spectrometer (Thermo Finnigan Delta V Advantage), which also gives ^{13}C -DOC values that can aid at interpreting the decomposition state and/or source (microbial vs plant) of organic matter (e.g. Dijkstra et al., 2006).

2.5. Statistical analyses

Statistical analyses and data visualisation were performed in R (version 4.1.1). First, the distribution of the variables (compound groups, C contents, and C/N) was tested for normality by means of a Shapiro-Wilk test, which indicated that not all variables were normally distributed. Therefore, differences in the relative abundance of these

variables were tested using the Kruskal Wallis test. The Dunn test with the Benjamin-Hochberg method was used as a post-hoc test to find which fractions are significantly different from each other. A difference was considered significant when $p < 0.05$.

The individual pyrolysis products were analysed by principal component analysis (PCA; Barré et al., 2018; Klein et al., 2022; Lopes-Mazzetto et al., 2018; Rovira and Grasset, 2019; Wang et al., 2016). PCA is an ordination technique to reduce the dataset to a few dimensions (i.e., new variables corresponding to a linear combination of the originals or principal components) that maximize the variance.

3. Results and discussion

3.1. Comparison of sample classes

The medians of the pyrolysis compound groups (Table 2) and other soil properties (Table 1) were compared for five samples classes, i.e., soil depth (0–5 cm vs 25–30 cm), forest type (deciduous vs spruce stands), soil process domain (Exchange vs Aluminium Domain), geological formation (Arlon vs Luxembourg), and SOM fraction (Bulk, POM, WEOM, BE, HA, FA). A significantly higher C content was found in the topsoil (3.5 %) compared to the subsoil (0.7 %) (Table 1). The amount of WEOM followed the total C content (C_{WEOM} , Table 1) and both were positively correlated ($r^2 = 0.88$), which is in agreement with other studies (Kaiser and Kalbitz, 2012; Kalks et al., 2020). A significant difference in C_{WEOM} was found for the topsoil between deciduous (77.3 mg/l) and coniferous (142.4 mg/l) stands (Table S3), confirming a higher influence of overstorey species close to the surface (Chuman et al., 2020; Girona-García et al., 2019; Grüneberg et al., 2014; Vesterdal et al., 2013). The relative amount of base-extractable SOM showed no significant differences for sample classes (C_{BE} , Table 1). The base-extractable fraction was the largest SOM pool, with medians reaching around 50 % for C_{BE} , while the relative amount of POM was around 20 % (Table 1). Soils under spruce showed a significantly higher relative contribution from POM (23.8 %) as compared to deciduous trees (22.5 %).

A significantly higher C/N and lower $\delta^{13}C_{WEOM}$ were observed in the topsoil as compared to the subsoil (Table 1), which confirms a larger relative contribution from microbial-derived material to the subsoil C (Šantrůčková et al., 2000; Sollins et al., 2009). A significant difference in

Table 2

Medians of compound groups for different sample classes, including fraction, soil depth, forest stand type, soil process domain and geological formation. The bold numbers indicate significant differences between the medians calculated by means of the Kruskal-Wallis test. For the fractions, the Dunn test was performed as a post-hoc. Fractions with the same letter are not significantly different from each other. Pyrolysis products that contribute to a group are given in Appendix A.

		Carbohydrates	Lignin products	N-containing compounds	Phenols	Aromatic products ^c
Fraction	POM	29.8 (b)	8.4 (c)	11.6 (b)	15.9 (a)	34.2 (b)
	WEOM	50.9 (ac)	0.5 (b)	22.6 (a)	6.3 (b)	15.2 (a)
	BE	47.4 (a)	2.9 (a)	25.1 (a)	10.5 (a)	14.4 (a)
	HA	30.3 (b)	5.7 (ac)	25.6 (a)	16.0 (a)	20.8 (a)
	FA	68.1 (c)	0.9 (b)	22.2 (a)	5.1 (b)	4.0 (c)
	Bulk	27.7 (b)	0.1 (b)	19.5 (a)	3.7 (b)	51.5 (b)
Soil depth ^a	Topsoil	42.3	5.5	14.5	14.0	15.8
	Subsoil	41.6	1.3	25.4	9.7	20.2
Forest stand type ^a	Deciduous	40.0	1.8	22.8	10.4	19.5
	Spruce	45.7	2.4	13.4	10.4	16.1
Soil process domain ^{a, b}	Aluminium	41.7	2.1	18.5	11.2	18.9
	Exchange	41.9	2.4	20.5	9.2	16.5
Geological formation ^a	Arlon	41.9	2.9	18.3	9.7	15.8
	Luxembourg	41.7	2.1	19.1	10.7	18.6

^a Medians were calculated without Bulk samples, due to the low reliability of the Bulk pyrograms (for an explanation see Section 3.2).

^b The soil process domain refers to the conditions before forest conversion, after conversion to spruce all plots shifted to the Aluminium Domain.

^c Aromatic products included benzenes, benzofurans, and PAHs.

C/N between forest types was only observed in the topsoil (C/N = 15.2 in deciduous and 22.8 in spruce, Table S3). This difference between forest types in the topsoil is indicative for a lower microbial activity in the topsoil under spruce, which might have amplified the effect of differences in litter quality on soil C/N (Cools et al., 2014).

Significant differences in the relative abundance of compound groups were found for all fractions (Table 2). The POM fraction showed a high relative abundance of lignin products, phenols, and aromatic products (i.e. benzenes, benzofurans and PAHs; Table 2), corroborating the general consensus that POM contains a high proportion of litter, roots, and charcoal (Christensen, 2001; von Lützow et al., 2007). The low relative contribution from lignin products and phenols in the WEOM

fraction reflects the low aqueous solubility of macromolecular lignin (Kaiser et al., 2004; Schellekens et al., 2017). A relative accumulation of N-containing compounds can be indicative of a higher contribution from microbial necromass (Kallenbach et al., 2016) and was evidenced in the WEOM and base-extractable fractions (BE, HA, FA). The BE and WEOM fractions were similar in relation to their high relative contribution from carbohydrates, N-containing compounds, and aromatic products, while they differed in relative abundance of lignin products and phenols for which the BE had values in between that of WEOM and POM. The HA fraction showed a higher contribution from lignin products, phenols, and aromatic products than FA, while the FA fraction had the highest contribution from carbohydrates (Table 2). A high relative abundance of

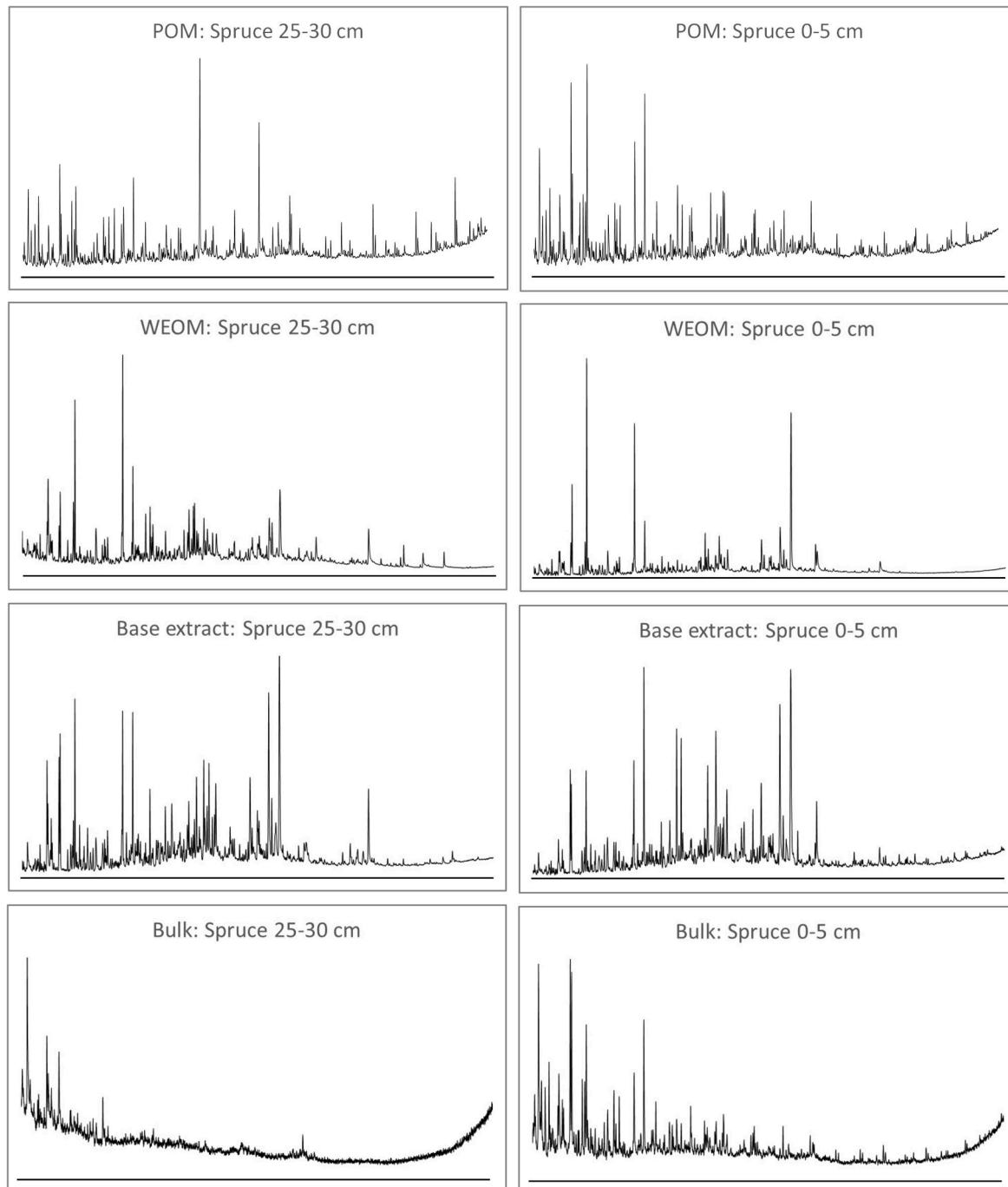


Fig. 2. Representative pyrograms of bulk mineral soil samples (Bulk) in comparison with organic fractions POM, WEOM, and BE for subsoil and topsoil of spruce forest soils (all are from plot 21).

carbohydrates in FA was also found by Preston et al. (1994), and could be related to their solubility in acid because of their high polarity (Saiz-Jimenez et al., 1979; Schnitzer and Khan, 1972). The compound groups in the pyrolysates from the Bulk samples showed the lowest relative abundance of lignin products (0.1 %) and phenols (3.7 %) and a high relative abundance of aromatic products (51.5 %, Table 2). This different composition in the Bulk samples compared to all organic fractions will be further discussed in Section 3.2.

The relative abundance of compound groups was further compared for soil depth, forest stand type, soil process domain, and geological formation in Table 2. Accordingly, deciduous stands had a significantly higher contribution from N-containing compounds than the coniferous ones, suggesting an increased proportion of plant material as a result of decreased microbial activity in spruce stands (Buresova et al., 2021). The differences between the geological formations and the soil process domains were not significant. Regarding soil depth, the relative contribution from lignin products was significantly higher in the topsoil while in the subsoil a significantly higher relative abundance of N-containing compounds was found. This difference probably reflects a higher relative contribution from plant- and microbial-derived material at the topsoil and subsoil, respectively. This interpretation is confirmed by C/N and $\delta^{13}\text{C}_{\text{WEOM}}$ (Table 1). A positive correlation between C/N and the total relative amount of N-containing compounds was found for the base- (i.e., BE, HA, FA; $0.81 < r^2 < 0.84$) and water-extractable (WEOM; $r^2 = 0.34$) fractions. The fact that such a correlation was not observed in the case of POM and Bulk samples ($r^2 < 0.03$) is probably inherent to the relatively intact plant material that makes up the POM fraction, and due to analytical constraints during pyrolysis of the mineral Bulk samples. Therefore, pyrolysates of the Bulk samples are discussed separately (Section 3.2).

3.2. Py-GC/MS of bulk mineral soil samples

The pyrograms of the bulk mineral soil compared to the SOM fractions showed large peaks at low RTs independently of soil depth and forest stand type, and their intensity rapidly decreased for molecules with higher RT (Figs. 2 and S2). Furthermore, 10 products, all with high RT, were absent from all the Bulk pyrolysates, and an additional 19 were absent from the Bulk pyrolysates of subsoil samples (Appendix A; Fig. S2). The few peaks with higher RT present in Bulk pyrolysates were all PAHs (Appendix A). The poor representation of compounds with higher RT in the Bulk pyrolysates thus disregarded a number of important molecular tracers, such as products from lignin (#26–38), cellulose (#22), and microbial material (#23–24, #40, #44–45; Appendix A) (e.g., Vancampenhout et al., 2016). Furthermore, the peak intensity was low (as visualised in comparison with the baseline in Fig. 2), with on average between 2 % and 10 % of that of the SOM fractions (calculated by the sum of all quantified peak areas before normalisation; Kaal et al., 2009). Increasing the amount of sample to the pyrolyser did not improve signal intensity.

The low signal intensity and the shift towards products of low molecular weight (MW) are typical outcomes of interactions between organic and inorganic components during the pyrolysis process (Eom et al., 2012; Wang et al., 2022). Reactive minerals such as clay, Ca, K, Fe and Al can cause rearrangements, cyclization and selective retention (Nierop and Van Bergen, 2002; Zegouagh et al., 2004) and explains the low relative abundance of lignin products (0.1 %) and the high relative abundance of aromatic products (51.5 %) (Table 2).

To test whether the molecular information provided by the Bulk samples was informative enough to interpret the effects of environmental processes on soil C in this sample set, a PCA was applied to the pyrolysates from the Bulk samples (Fig. S3). The scores showed an effect of soil depth on PC1 (with exception of three deciduous topsoil samples), and, independently of soil depth, a strong clustering according to plot (PC2–PC4) and thus to lithological differences in the mineral fraction of those samples. The loadings showed that this plot clustering was caused

by a separation of low MW aromatic products (benzenes) and lignin products on PC1, and high positive loadings of aromatic products on PC2 and PC3 (Fig. S3a, b).

Thus, the arguments given in Section 3.1 on the relative contribution from lignin products (lowest) and aromatic products (highest) (Table 2) together with the strong plot clustering in PCA (Fig. S3) and the absence of many products with high MW in Bulk pyrolysates (Appendix A), suggest a dominant influence of the mineral matrix on Bulk pyrolysates. Using THM-TMAH, Brock et al. (2019) also observed a dominance of plot location on the content and composition of cutin, suberin and lignin, using bulk mineral soil samples from plots in the Gaume and Luxembourg (including our plots 8, 12, 25 and 36; Table S2). Such location effects were absent in the first four principal components of the PCA applied to the organic SOM fractions (see Sections 3.3 and 3.4). This suggests that, although THM-TMAH is less sensitive for catalyst effects than pyrolysis without methylation (Py-GC/MS), mineral-induced reactions in pyrolysis methods obtained from bulk mineral soil samples may confound the ecological interpretations for samples collected from soils on different parent materials and taken at different depths.

3.3. Soil process recognition by PCA applied to pyrolysates of organic SOM fractions

A detailed multivariate interpretation of differences in molecular composition in the organic SOM fractions was performed by PCA. The shared variation of all pyrolysis products in the loadings was used to interpret the process reflected by each individual component. Thereafter, this interpretation was used to evaluate the relative effects (Klein et al., 2022) of soil depth, decomposition, and litter input material for the different SOM fractions (Section 3.4). The first four components explained more than 71 % of the total variance of the dataset. The projections of the scores and loadings are given in Fig. 3.

3.3.1. Identification of the main trends using PCA loadings

Most carbohydrates and some N-containing compounds (#40, #44–46, #48–49) had negative loadings on PC1. Pyrolysis products with high positive loadings on PC1 (Fig. 3a) are indicative of plant (lignin products) and burnt (benzenes, benzofurans, and PAHs; Kaal et al., 2009; Morf et al., 2002) materials, thus sharing aromatic macromolecules as their source.

Pyrolysis products with negative loadings on PC2 include lignin-derived products, catechol derived from tannin (#64; Galletti and Reeves, 1992), and levoglucosan derived from cellulose (#22; Pouwels et al., 1989), which are all hydrophobic plant macromolecules (Kaiser et al., 2004). On the other hand, the combination of pyrolysis products with positive loadings on PC2 has been linked to hydrophilic materials (Schellekens et al., 2017), including products with low MW (#1, #14–17) as well as those with polar functional groups, such as ketones (#8, #10, #14–15) and aldehydes (e.g., #16–17, #19), and heterocyclic aromatic hydrocarbons (#11–13, #43; Appendix A). Thus, PC2 likely reflects the aqueous solubility of SOM.

PC3 separates N-containing compounds (#39–52, positive loadings) from lignin products (#26–38, negative) (Fig. 3b), a difference commonly interpreted to reflect contributions from microbial and plant biomass, respectively (see Section 3.1). Within the lignin group, the highest negative loadings on PC3 were found for moieties with a C₃ alkyl side chain (#30, #37) and 4-vinylguaiacol (#29) that are indicative for relatively intact lignin (Nierop et al., 2001; van der Hage et al., 1993) whereas corresponding moieties with an oxygenated alkyl side chain (#31, #38) have low negative or positive loadings and reflect degraded lignin (Nierop et al., 1999). The combination of more transformed plant material and a relatively higher contribution from microbial material suggests that PC3 reflects the degree of SOM decomposition.

PC4 clearly separated the lignin products into two groups (Fig. 3b): all guaiacyl products had positive loadings (#26–32) along this axis, while syringyl products had negative ones (#33–38). Guaiacyl and

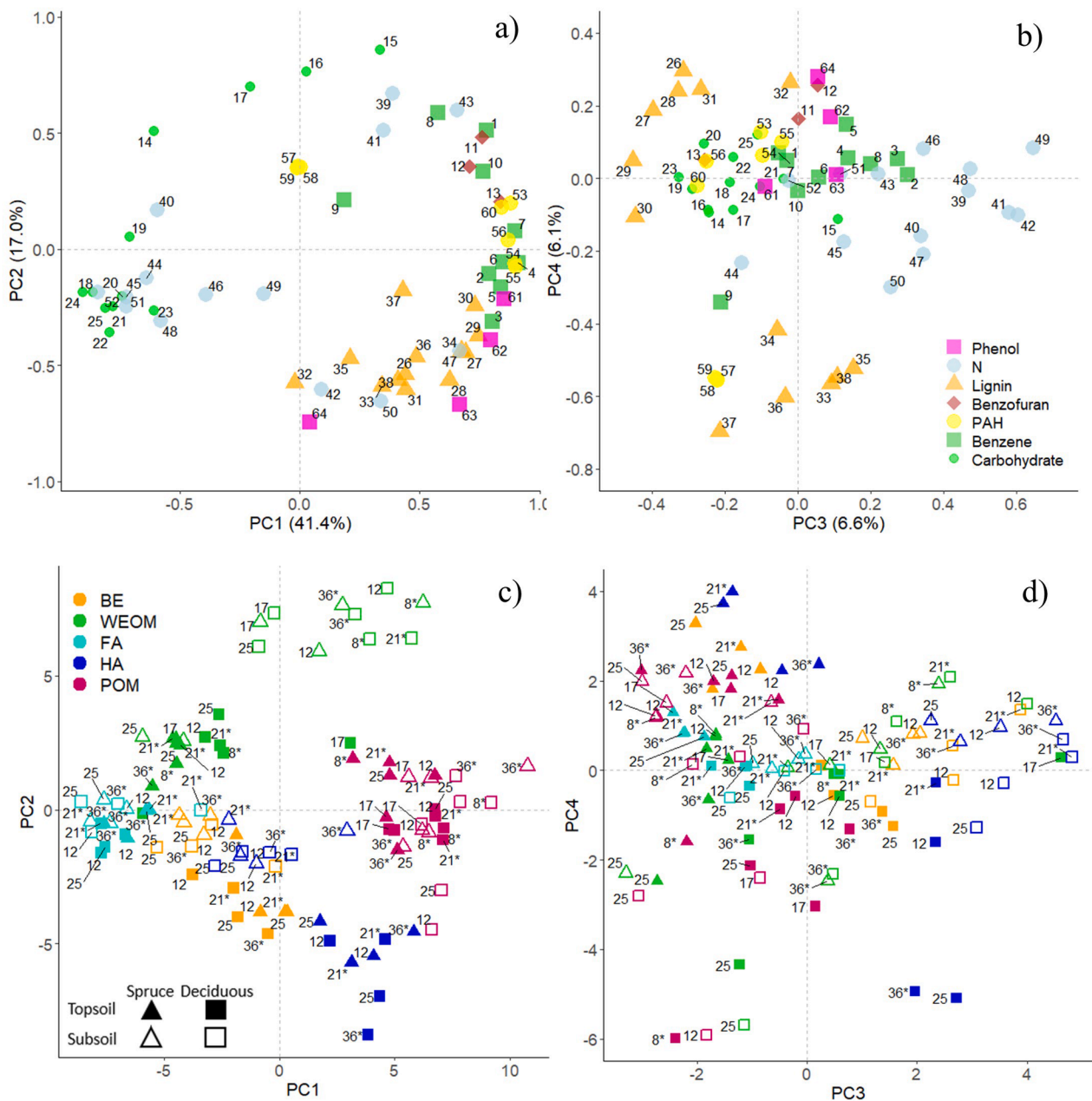


Fig. 3. Loadings (a, b) and scores (c, d) of the PC1–PC2 and PC3–PC4 projections from PCA applied to all samples from the SOM fractions. Pyrolysis products that correspond to the codes in the loadings are given in the [Appendix A](#). For the scores, SOM fraction and soil depth clearly group on PC1–PC2 but are scattered in PC3–PC4 projection. More detail on trends in PC3–PC4 projection is given in [Fig. 4](#). The asterisk behind the plot numbers indicates that the soil is on the Aluminium Domain; note that the soil process domain under spruce refers to the conditions before forest stand conversion.

syringyl lignin is often used to infer the origin of the plant input material, as deciduous species contain both lignin types while in coniferous species mainly guaiacyl is found ([Hedges and Mann, 1979](#); [Thevenot et al., 2010](#)). The separation of products thus suggests that PC4 reflects input material, i.e., deciduous vs spruce.

3.3.2. Compositional differences between the different SOM fractions by PCA scores

The clear clustering of SOM fractions in the PC1–PC2 scores projection highlights the dominant influence of the SOM fractionation method on its molecular composition ([Fig. 3c](#)), which was also evident by the significant difference in the relative abundance of chemical groups ([Table 2](#)).

The POM samples had the highest positive scores on PC1 of all

fractions, and predominantly negative scores on PC3 ([Fig. 3c, d](#)). For PC1 this reflects its operational character, i.e., it isolates the light fraction that mainly consists of plant fragments and charcoal, thereby explaining the grouping of lignin and aromatic products ([Fig. 3a](#), [Table 2](#)). The negative scores on PC3 reflect that the light fraction represents relative intact SOM (i.e., plant material) in comparison with the total SOM pool. On both components the POM was associated with high relative contribution from lignin products and low relative contribution from N-containing compounds ([Table 2](#)).

Regarding the base-extractable fractions, the BE was evidently situated in between HA and FA on PC1 to PC3. The FA showed the lowest variation and was associated with carbohydrates on PC1 and PC3, which is in line with the high solubility of those compounds in acids. The HA, on the other hand, was associated with a larger contribution from lignin

products on both PC1 and PC2 (Fig. 2; Table 2). This compositional difference between HA and FA in terms of lignin and carbohydrates is already well established in the literature (Keeler et al., 2006; Preston et al., 1994).

In addition to the obvious link between hydrophilic compounds and the WEOM on PC2 (Fig. 3a), the WEOM showed the largest variation of all SOM fractions in all principal components (Fig. 3c, d). This is in agreement with previous results of similar fractions obtained from tropical forest soils (Barreto et al., 2021) and may reflect the dynamic and temporal nature of WEOM, as dissolved organic matter is easily reworked by microbes and continuously precipitates and sorbs on soil components (Kaiser and Kalbitz, 2012; Roth et al., 2019).

3.4. Ecological information enclosed in the different SOM fractions by PCA scores

To evaluate how decomposition and input material were expressed in each SOM fraction, the scores of PC3 and PC4 are also presented individually (Fig. 4). This graphical representation allows the identification of consistent trends, even if averages are not significantly different. Similarly, differences between top- and subsoil are visualised in Fig. S4.

3.4.1. Molecular changes with soil depth

All SOM fractions showed consistent differences between top- and subsoil samples on PC1, PC2 and/or PC3 (Figs. 3c, d and S4). On PC1, a consistent difference between top- and subsoil was exclusively observed in the HA fraction, with more positive scores for topsoil samples compared to the corresponding subsoil samples (Fig. S4a). This reflects a larger proportion of aromatic macromolecules (and/or lower proportion of carbohydrates) in the HA of the topsoil samples (Fig. 3a). In contrast, the WEOM generally showed more positive scores for subsoil samples on PC1 (Fig. S4a), which can be explained by increased oxidation and fragmentation of macromolecules in the subsoil that increases their hydrophilicity (Crawford and Crawford, 1984; Guggenberger et al., 1994). These differences between the WEOM and the base-extractable fractions is explained by the alkaline conditions during extraction of the latter that increase the polarity of macromolecules such as lignin via

deprotonation of acidic functional groups.

A shift according to soil depth indicated by PC2 was consistent for all SOM fractions with more negative values for the topsoil (Fig. S4b), and highlights the importance of influx or generation of hydrophilic SOM in the subsoil (Guggenberger et al., 1994; Toosi et al., 2012). The shift was clearly observed in the WEOM, BE and HA, less pronounced in the FA, and absent in the POM fraction.

Except for the POM, all fractions showed more positive scores on PC3 for the subsoil, reflecting the expected lower proportion of plant material and increased SOM decomposition with depth (Fig. S4c). The opposite trend in the POM fraction (consistently more positive scores for topsoil samples) likely reflects slower decomposition in the subsoil, e.g. due to nutrient and oxygen constraints (Six et al., 2002). This may also explain the absence of differences between top- and subsoil in the of POM on the other PCs (Figs. 3c, d and S4a–d), and reflects the property of POM being relatively undecomposed.

3.4.2. Molecular information related to decomposition evaluated by PC3 scores

PC3 showed a clear and consistent shift between the topsoil and the subsoil reflecting an increased degree of decomposition with depth as discussed in Section 3.4.1. To evaluate the effect of forest stand type on SOM decomposition, PC3 scores are compared separately for top- and subsoil (Fig. 4a, b).

In the topsoil, the difference between broadleaved and coniferous stands was clearly evidenced on PC3 (Fig. 4a), indicating a slower SOM decomposition in the topsoil under spruce stands (Buresova et al., 2021; Desie et al., 2021; Hansson et al., 2013; Vesterdal et al., 2008). The POM and FA fractions showed little difference between forest stand types. This is explained by their operational fractionation procedure that results in a relatively homogenous but specific SOM pool in terms of decomposition, consisting mainly of plant fragments (POM) or carbohydrates and N-containing compounds (FA).

In the subsoil, the effect of forest type on PC3 was less evident and both coniferous and deciduous stands displayed similar scores for samples from corresponding plots, which reflects that the influence of forest type on SOM decomposition decreases in deeper soil layers (Brock et al., 2019; Chuman et al., 2020; Cools et al., 2014; Grüneberg et al., 2014).

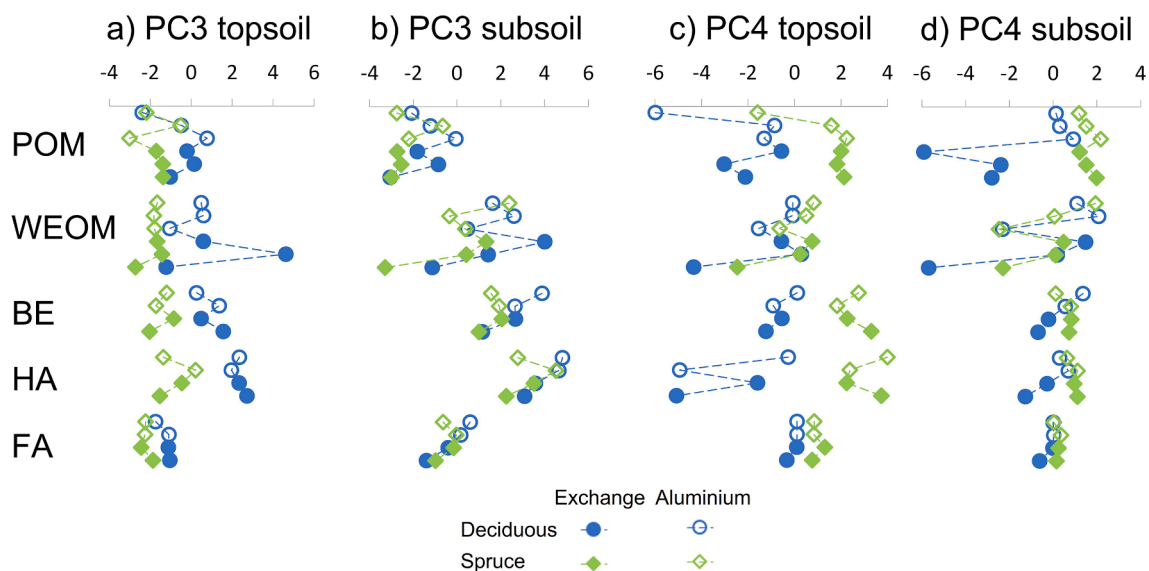


Fig. 4. Scores of PC3–PC4 presented individually for subsoil and topsoil to visualise differences between forest stand type. The corresponding loadings are given in Fig. 3b. The scores are the same as those in Fig. 3d, but presented differently. With this alternative presentation of scores, differences and similarities in ecological factors are visualised between SOM fractions (i.e., to which extend are ecological factors expressed in the SOM fractions?). PC3 and PC4 reflected SOM decomposition state and input material, respectively. Note that the soil process domain under spruce refers to the conditions before forest stand conversion. Samples were connected with dotted lines to better visualise trends.

This decrease in influence of forest type with soil depth can be attributed to the transformation of SOM into microbial necromass (Prescott and Vesterdal, 2021). Alternatively, the effect of forest conversion may not yet have affected SOM composition at 25–30 cm depth.

3.4.3. Molecular information related to differences in litter input by PCA scores

In the topsoil, samples from spruce stands had more positive scores on PC4 than corresponding deciduous samples (except for WEOM) (Fig. 4c). This is in agreement with a dominant effect of forest type on the composition of plant-derived SOM obtained with THM-TMAH as found previously for this site by Brock et al. (2019), and with the traditional use of the syringyl/guaiacyl lignin ratio in SOM as a source indicator (Hedges and Mann, 1979; Thevenot et al., 2010). The fact that forest stand type was not reflected in the WEOM lignin composition is explained by the low aqueous solubility of macromolecular lignin.

In the subsoil, the difference between deciduous and spruce was not evident, except in the POM fraction (Fig. 4d). This can be explained by a larger contribution from roots to subsoil SOM, as syringyl/guaiacyl ratios are considerably lower for roots compared to leaves and needles (Brock et al., 2019). Another explanation could be the predominant control of decomposition on SOM composition in the subsoil (Fig. 4b), because syringyl lignin is preferentially decomposed over guaiacyl lignin (Thevenot et al., 2010). The fact that the difference between spruce and deciduous stands was only evident in the least decomposed fraction (i.e., the POM; Fig. 4d), together with the similar values for top- and subsoil in the POM (Fig. S4d), supports a decomposition effect on the lignin source signal, since the degree of SOM decomposition increases with soil depth (Rumpel and Kögel-Knabner, 2011).

3.4.4. Molecular information related to soil process domain

In Fig. 4 open symbols represent the plots that were classified as belonging to the Exchange Domain prior to conversion, while closed symbols represent samples from plots already belonging to the Aluminium Domain before conversion. After conversion to spruce, all stands that were still in the Exchange Domain under deciduous forest, shifted to the Aluminium Domain (Desie et al., 2021, 2019). A consistent effect of the soil process domain was exclusively present in the subsoil on PC4 (Fig. 4): In the POM and, to a lesser extent, the HA and BE, the deciduous forest samples from the Exchange Domain were clearly separated from those belonging to the Aluminium Domain, whereas the samples from spruce all showed positive scores and low variation (Fig. 4d).

Therefore, the shift in below-ground stable state that occurs when plots acidify and move from the Exchange Domain to the Aluminium Domain as a result of conversion (Brock et al., 2019; Desie et al., 2019), was most clearly observed in the subsoil at a molecular level. This observation was limited to those SOM fractions with relatively large contributions from plant material as indicated by lignin products (average proportions between 2.9 % and 8.4 % for POM, HA and BE, and between 0.5 % and 0.9 % for WEOM and FA, Table 2). Thus, the effect of soil process domain corroborates the vertical decoupling that occurs when burrowing soil fauna disappears due to conversion to the Aluminium Domain, and no longer incorporates leaf litter into the subsoil (Desie et al., 2019). For deciduous plots that were already in the Aluminium Domain, this change in SOM composition was not observed because bioturbation was already low prior to conversion.

4. Conclusions

In this study, we used a reverse fit approach to systematically compare several commonly used operationally defined SOM fractions to evaluate their ability to detect changes in below-ground functioning after forest conversion.

Pyrograms of bulk mineral soil samples did not prove to be reliable for studying the effects of forest stand conversion on SOM composition

in the study area because of low signal intensity and a shift towards unspecific low MW pyrolysis products.

The fractionation method had a determining impact on relative abundances of compound groups, but Py-GC/MS of SOM fractions obtained by alkaline extraction (BE, HA, FA) and without it (WEOM, POM) provided the same molecules and coherent shifts in terms of decomposition, litter input material, and changes in acidity. This indicates that potential chemical alteration due to alkaline conditions as proposed by Lehmann and Kleber (2015) did not hinder environmental interpretations.

Overall, effects related to soil depth were observed in all SOM fractions. Effects of input material were not identified in the WEOM fraction, were evident in the topsoil for base-extractable fractions (HA, FA, BE), and equally expressed in both top- and subsoil for the POM. SOM decomposition state was expressed in all SOM fractions, except for the POM. Thus, although the amount of POM may reflect the degree of decomposition of soil C, its molecular composition mainly provided information on tree species. The effect of a shift in soil process domain was more pronounced in the POM, and to a lesser extent in the HA and BE fractions, but absent from the FA and WEOM. We therefore conclude that BE and HA provided the most comprehensive environmental and ecological interpretation of soil C, while POM highlighted C dynamics and soil process domain. Ultimately the choice of fraction(s) thus depends on the research question.

Declaration of Competing Interest

The authors declare that they have no known competing financial interests or personal relationships that could have appeared to influence the work reported in this paper.

Data availability

Data will be made available on request.

Acknowledgements

This research was financially supported by the Flanders Research Foundation (FWO): by a FWO Fellowship Grant awarded to J.S. (12ZY320N/SW) and an FWO Fundamental Research Grant to K.V.C. and J.S. (ZKD9914-01-W01). We thank Kim Vekemans for the support in the laboratory. We thank the municipal councils of Virton and Etalle and B. Van Doren of the Cantonnement de Virton of the Walloon Department of Nature and Forest for their support. Furthermore, we thank two anonymous reviewers for their critical and detailed view.

Appendix B. Supplementary data

Supplementary data to this article can be found online at <https://doi.org/10.1016/j.geoderma.2022.116280>.

References

- Barré, P., Quénéa, K., Vidal, A., Cécillon, L., Christensen, B.T., Kätterer, T., Macdonald, A., Petit, L., Plante, A.F., van Oort, F., Chenu, C., 2018. Microbial and plant-derived compounds both contribute to persistent soil organic carbon in temperate soils. *Biogeochemistry* 140, 81–92. <https://doi.org/10.1007/s10533-018-0475-5>.
- Barreto, M.S.C., Schellekens, J., Ramlogan, M., Rouff, A.A., Elzinga, E.J., Vidal-Torrado, P., Alleoni, L.R.F., 2021. Effects of horticulture on soil organic matter properties in highly weathered tropical soils. *Soil Tillage Res.* 213, 105156 <https://doi.org/10.1016/j.still.2021.105156>.
- Brock, O., Kooijman, A., Nierop, K.G.J., Muys, B., Vancampenhout, K., Jansen, B., 2019. Organic geochemistry disentangling the effects of parent material and litter input chemistry on molecular soil organic matter composition in converted forests in Western Europe. *Org. Geochem.* 134, 66–76. <https://doi.org/10.1016/j.orggeochem.2019.05.006>.
- Brock, O., Kalbitz, K., Absalah, S., Jansen, B., 2020. Effects of development stage on organic matter transformation in Podzols. *Geoderma* 378, 114625. <https://doi.org/10.1016/j.geoderma.2020.114625>.

- Buresova, A., Tejnecky, V., Kopecky, J., Drabek, O., Madrova, P., Rerichova, N., Omelka, M., Krizova, P., Nemecek, K., Parr, T.B., Ohno, T., Sagova-Mareckova, M., 2021. Litter chemical quality and bacterial community structure influenced decomposition in acidic forest soil. *Eur. J. Soil Biol.* 103, 103271 <https://doi.org/10.1016/j.ejsobi.2020.103271>.
- Buurman, P., Peterse, F., Almendros Martin, G., 2007. Soil organic matter chemistry in alluvial soils: a pyrolysis-GC/MS study of a Costa Rican Andosol catena. *Eur. J. Soil Sci.* 58, 1330–1347. <https://doi.org/10.1111/j.1365-2389.2007.00925.x>.
- Buurman, P., Roscoe, R., 2011. Different chemical composition of free light, occluded light and extractable SOM fractions in soils of Cerrado and tilled and untilled fields, Minas Gerais, Brazil: a pyrolysis-GC/MS study. *Eur. J. Soil Sci.* 62, 253–266. <https://doi.org/10.1111/j.1365-2389.2010.01327.x>.
- Carr, A.S., Boom, A., Chase, B.M., Roberts, D.L., Roberts, Z.E., 2010. Molecular fingerprinting of wetland organic matter using pyrolysis-GC/MS: an example from the southern Cape coastline of South Africa. *J. Paleolimnol.* 44, 947–961. <https://doi.org/10.1007/s10933-010-9466-9>.
- Carrington, E.M., Hernes, P.J., Dyda, R.Y., Plante, A.F., Six, J., 2012. Biochemical changes across a carbon saturation gradient: lignin, cutin, and suberin decomposition and stabilization in fractionated carbon pools. *Soil Biol. Biochem.* 47, 179–190. <https://doi.org/10.1016/j.soilbio.2011.12.024>.
- Chiapini, M., Schellekens, J., Calegari, M.R., de Almeida, J.A., Buurman, P., de Camargo, P.B., Vidal-Torrado, P., 2018. Formation of black carbon rich 'sombri' horizons in the subsoil – a case study from subtropical Brazil. *Geoderma* 314, 232–244. <https://doi.org/10.1016/j.geoderma.2017.10.031>.
- Christensen, B.T., 2001. Physical fractionation of soil and structural and functional complexity in organic matter turnover. *Eur. J. Soil Sci.* 52, 345–353. <https://doi.org/10.1046/j.1365-2389.2001.00417.x>.
- Chuman, T., Oulehle, F., Zajíčková, K., Hruška, J., 2020. The legacy of acidic deposition controls soil organic carbon pools in temperate forests across the Czech Republic. *Eur. J. Soil Sci.* 1–22. <https://doi.org/10.1111/ejss.13073>.
- Cools, N., Vesterdal, L., De Vos, B., Vanguelova, E., Hansen, K., 2014. Tree species is the major factor explaining C:N ratios in European forest soils. *For. Ecol. Manage.* 311, 3–16. <https://doi.org/10.1016/j.foreco.2013.06.047>.
- Crawford, R.L., Crawford, D.L., 1984. Recent advances in studies of the mechanisms of microbial degradation of lignins. *Enzyme Microb. Technol.* 6, 434–442. [https://doi.org/10.1016/0141-0229\(84\)90092-9](https://doi.org/10.1016/0141-0229(84)90092-9).
- Denis, M., Jeanneau, L., Pierson-Wickman, A.-C., Humbert, G., Petitjean, P., Jaffrézic, A., Gruau, G., 2017. A comparative study on the pore-size and filter type effect on the molecular composition of soil and stream dissolved organic matter. *Org. Geochem.* 110, 36–44. <https://doi.org/10.1016/j.orggeochem.2017.05.002>.
- Desie, E., Vancampenhout, K., Heyens, K., Hlava, J., Verheyen, K., Muys, B., 2019. Forest conversion to conifers induces a regime shift in soil process domain affecting carbon stability. *Soil Biol. Biochem.* 136, 107540.
- Desie, E., Muys, B., Jansen, B., Vesterdal, L., Vancampenhout, K., 2021. Pedogenic threshold in acidity explains context-dependent tree species effects on soil carbon. *Front. For. Glob. Chang.* 4, 1–9. <https://doi.org/10.3389/ffgc.2021.679813>.
- Dijkstra, P., Ishizu, A., Doucet, R., Hart, S.C., Schwartz, E., Menyailo, O.V., Hungate, B. A., 2006. ¹³C and ¹⁵N natural abundance of the soil microbial biomass. *Soil Biol. Biochem.* 38, 3257–3266. <https://doi.org/10.1016/j.soilbio.2006.04.005>.
- Eom, I.-Y., Kim, J.-Y., Kim, T.-S., Lee, S.-M., Choi, D., Choi, I.-G., Choi, J.-W., 2012. Effect of essential inorganic metals on primary thermal degradation of lignocellulosic biomass. *Bioreour. Technol.* 104, 687–694. <https://doi.org/10.1016/j.biortech.2011.10.035>.
- Filep, T., Zacháry, D., Jakab, G., Szalai, Z., 2022. Chemical composition of labile carbon fractions in Hungarian forest soils: insight into biogeochemical coupling between DOM and POM. *Geoderma* 419, 115867. <https://doi.org/10.1016/j.geoderma.2022.115867>.
- Galletti, G.C., Reeves, J.B., 1992. Pyrolysis/gas chromatography/ion-trap detection of polyphenols (vegetable tannins): preliminary results. *Org. Mass Spectrom.* 27, 226–230. <https://doi.org/10.1002/oms.1210270313>.
- Girona-García, A., Badía-Villas, D., Jiménez-Morillo, N.T., González-Pérez, J.A., 2019. Changes in soil organic matter composition after Scots pine afforestation in a native European beech forest revealed by analytical pyrolysis (Py-GC/MS). *Sci. Total Environ.* 691, 1155–1161. <https://doi.org/10.1016/j.scitotenv.2019.07.229>.
- Grüneberg, E., Ziche, D., Wellbrock, N., 2014. Organic carbon stocks and sequestration rates of forest soils in Germany. *Glob. Chang. Biol.* 20, 2644–2662. <https://doi.org/10.1111/gcb.12558>.
- Guggenberger, G., Zech, W., Schulten, H.R., 1994. Formation and mobilization pathways of dissolved organic matter: evidence from chemical structural studies of organic matter fractions in acid forest floor solutions. *Org. Geochem.* 21, 51–66. [https://doi.org/10.1016/0146-6380\(94\)90087-6](https://doi.org/10.1016/0146-6380(94)90087-6).
- Han, L., Wang, Y., Xu, Y., Wang, Y., Zheng, Y., Wu, J., 2021. Water- and base-extractable organic matter in sediments from lower Yangtze River–Estuary–East China Sea continuum: insight into accumulation of organic carbon in the river-dominated margin. *Front. Mar. Sci.* 8 <https://doi.org/10.3389/fmars.2021.617241>.
- Hansson, K., Fröberg, M., Helmisaari, H.S., Kleja, D.B., Olsson, B.A., Olsson, M., Persson, T., 2013. Carbon and nitrogen pools and fluxes above and below ground in spruce, pine and birch stands in southern Sweden. *For. Ecol. Manage.* 309, 28–35. <https://doi.org/10.1016/j.foreco.2013.05.029>.
- Hedges, J.I., Mann, D.C., 1979. The characterization of plant tissues by their lignin oxidation products. *Geochim. Cosmochim. Acta* 43, 1803–1807. [https://doi.org/10.1016/0016-7037\(79\)90028-0](https://doi.org/10.1016/0016-7037(79)90028-0).
- IUSS Working Group WRB, 2015. In: World Reference Base for Soil Resources 2014, Update 2015. International Soil Classification System for Naming Soils and Creating Legends for Soil Maps, World Soil Resources Reports No. 106. FAO, Rome. <https://doi.org/10.1038/nnano.2009.216>.
- Justi, M., Schellekens, J., de Camargo, P.B., Vidal-Torrado, P., 2017. Long-term degradation effect on the molecular composition of black carbon in Brazilian Cerrado soils. *Org. Geochem.* 113, 196–209. <https://doi.org/10.1016/j.orggeochem.2017.06.002>.
- Kaal, J., Martínez Cortizas, A., Nierop, K.G.J., 2009. Characterisation of aged charcoal using a coil probe pyrolysis-GC/MS method optimised for black carbon. *J. Anal. Appl. Pyrol.* 85, 408–416. <https://doi.org/10.1016/j.jaap.2008.11.007>.
- Kaal, J., Cortizas, A.M., Biester, H., 2017. Downstream changes in molecular composition of DOM along a headwater stream in the Harz mountains (Central Germany) as determined by FTIR, Pyrolysis-GC-MS and THM-GC-MS. *J. Anal. Appl. Pyrol.* 126, 50–61. <https://doi.org/10.1016/j.jaap.2017.06.025>.
- Kaiser, K., Guggenberger, G., Haumaier, L., 2004. Changes in dissolved lignin-derived phenols, neutral sugars, uronic acids, and amino sugars with depth in forested Haplic Arenosols and Rendzic Leptosols. *Biogeochemistry* 70, 135–151. <https://doi.org/10.1023/B:Biog.0000049340.77963.18>.
- Kaiser, K., Kalbitz, K., 2012. Cycling downwards – dissolved organic matter in soils. *Soil Biol. Biochem.* 52, 29–32. <https://doi.org/10.1016/j.soilbio.2012.04.002>.
- Kalks, F., Liebmann, P., Wordell-Dietrich, P., Guggenberger, G., Kalbitz, K., Mikutta, R., Helfrich, M., Don, A., 2020. Fate and stability of dissolved organic carbon in topsoils and subsoils under beech forests. *Biogeochemistry* 148, 111–128. <https://doi.org/10.1007/s10533-020-00649-8>.
- Kallenbach, C.M., Frey, S.D., Grandy, A.S., 2016. Direct evidence for microbial-derived soil organic matter formation and its ecophysiological controls. *Nat. Commun.* 7 <https://doi.org/10.1038/ncomms13630>.
- Keeler, C., Kelly, E.F., Maciel, G.E., 2006. Chemical-structural information from solid-state ¹³C NMR studies of a suite of humic materials from a lower montane forest soil, Colorado, USA. *Geoderma* 130, 124–140. <https://doi.org/10.1016/j.geoderma.2005.01.015>.
- Kleber, M., Lehmann, J., 2019. Humic substances extracted by alkali are invalid proxies for the dynamics and functions of organic matter in terrestrial and aquatic ecosystems. *J. Environ. Qual.* 48, 207–216. <https://doi.org/10.2134/jeq2019.01.0036>.
- Klein, K., Schellekens, J., Groß-Schmolders, M., von Sengbusch, P., Alewell, C., Leifeld, J., 2022. Characterizing ecosystem-driven chemical composition differences in natural and drained Finnish bogs using pyrolysis-GC/MS. *Org. Geochem.* 165, 104351.
- Kögel-Knabner, I., 2000. Analytical approaches for characterizing soil organic matter. *Org. Geochem.* 31, 609–625. [https://doi.org/10.1016/S0146-6380\(00\)00042-5](https://doi.org/10.1016/S0146-6380(00)00042-5).
- Lavallee, J.M., Soong, J.L., Cotrufo, M.F., 2020. Conceptualizing soil organic matter into particulate and mineral-associated forms to address global change in the 21st century. *Glob. Chang. Biol.* 26, 261–273. <https://doi.org/10.1111/gcb.14859>.
- Lehmann, J., Kleber, M., 2015. The contentious nature of soil organic matter. *Nature* 528, 60–68. <https://doi.org/10.1038/nature16069>.
- Lopes-Mazzetto, J.M., Schellekens, J., Vidal-Torrado, P., Buurman, P., 2018. Impact of drainage and soil hydrology on sources and degradation of organic matter in tropical coastal podzols. *Geoderma* 330, 79–90. <https://doi.org/10.1016/j.geoderma.2018.05.015>.
- Man, M., Pierson, D., Chiu, R., Tabatabaei Anaraki, M., vandenEnden, L., Ye, R.X., Lajtha, K., Simpson, M.J., 2022. Twenty years of litter manipulation reveals that above-ground litter quantity and quality controls soil organic matter molecular composition. *Biogeochemistry* 159 (3), 393–411.
- Morf, P., Hasler, P., Nussbaumer, T., 2002. Mechanisms and kinetics of homogeneous secondary reactions of tar from continuous pyrolysis of wood chips. *Fuel* 81, 843–853. [https://doi.org/10.1016/S0016-2361\(01\)00216-2](https://doi.org/10.1016/S0016-2361(01)00216-2).
- Nierop, K.G.J., Buurman, P., 1998. Composition of soil organic matter and its water-soluble fraction under young vegetation on drift sand, central Netherlands. *Eur. J. Soil Sci.* 49, 605–615. <https://doi.org/10.1046/j.1365-2389.1998.4940605.x>.
- Nierop, K.G.J., Buurman, P., de Leeuw, J.W., 1999. Effect of vegetation on chemical composition of H horizons in incipient podzols as characterized by NMR and pyrolysis-GC/MS. *Geoderma* 90, 111–129. [https://doi.org/10.1016/S0016-7061\(98\)00095-0](https://doi.org/10.1016/S0016-7061(98)00095-0).
- Nierop, K.G.J., Van Bergen, P.F., 2002. Clay and ammonium catalyzed reactions of alkanols, alkanolic acids and esters under flash pyrolytic conditions. *J. Anal. Appl. Pyrol.* 63, 197–208. [https://doi.org/10.1016/S0165-2370\(01\)00154-1](https://doi.org/10.1016/S0165-2370(01)00154-1).
- Nierop, K.G.J., van Lagen, B., Buurman, P., 2001. Composition of plant tissues and soil organic matter in the first stages of a vegetation succession. *Geoderma* 100, 1–24. [https://doi.org/10.1016/S0016-7061\(00\)00078-1](https://doi.org/10.1016/S0016-7061(00)00078-1).
- Olk, D.C., Bloom, P.R., Perdue, E.M., McKnight, D.M., Chen, Y., Farenhorst, A., Senesi, N., Chin, Y.-P., Schmitt-Kopplin, P., Hertkorn, N., Harir, M., 2019. Environmental and agricultural relevance of humic fractions extracted by alkali from soils and natural waters. *J. Environ. Qual.* 48, 217–232. <https://doi.org/10.2134/jeq2019.02.0041>.
- Pouwels, A.D., Eijkel, G.B., Boon, J.J., 1989. Curie-point pyrolysis-capillary gas chromatography-high-resolution mass spectrometry of microcrystalline cellulose. *J. Anal. Appl. Pyrol.* 14, 237–280. [https://doi.org/10.1016/0165-2370\(89\)80003-8](https://doi.org/10.1016/0165-2370(89)80003-8).
- Prescott, C.E., Vesterdal, L., 2021. Decomposition and transformations along the continuum from litter to soil organic matter in forest soils. *For. Ecol. Manage.* 498, 119522. <https://doi.org/10.1016/j.foreco.2021.119522>.
- Preston, C.M., Hempfling, R., Schulten, H.R., Schnitzer, M., Trofymow, J.A., Axelson, D. E., 1994. Characterization of organic matter in a forest soil of coastal British Columbia by NMR and pyrolysis-field ionization mass spectrometry. *Plant Soil* 158, 69–82. <https://doi.org/10.1007/BF00007919>.
- Roscoe, R., Buurman, P., 2003. Tillage effects on soil organic matter in density fractions of a Cerrado Oxisol. *Soil Tillage Res.* 70, 107–119. [https://doi.org/10.1016/S0167-1987\(02\)00160-5](https://doi.org/10.1016/S0167-1987(02)00160-5).

- Roth, V.N., Lange, M., Simon, C., Hertkorn, N., Bucher, S., Goodall, T., Griffiths, R.I., Mellado-Vázquez, P.G., Mommer, L., Oram, N.J., Weigelt, A., Dittmar, T., Gleixner, G., 2019. Persistence of dissolved organic matter explained by molecular changes during its passage through soil. *Nat. Geosci.* 12, 755–761. <https://doi.org/10.1038/s41561-019-0417-4>.
- Rovira, P., Grasset, L., 2019. Plant versus microbial signature in densimetric fractions of Mediterranean forest soils: a study by thermochemolysis gas chromatography mass spectrometry. *J. Soil. Sediment.* 19, 58–72. <https://doi.org/10.1007/s11368-018-2046-8>.
- Rumpel, C., Kögel-Knabner, I., 2011. Deep soil organic matter—a key but poorly understood component of terrestrial C cycle. *Plant Soil* 338, 143–158. <https://doi.org/10.1007/s11104-010-0391-5>.
- Saiz-Jimenez, C., Haider, K., Meuzelaar, H.L.C., 1979. Comparisons of soil organic matter and its fractions by pyrolysis mass-spectrometry. *Geoderma* 22, 25–37. [https://doi.org/10.1016/0016-7061\(79\)90037-5](https://doi.org/10.1016/0016-7061(79)90037-5).
- Šantrůčková, H., Bird, M.I., Lloyd, J., 2000. Microbial processes and carbon-isotope fractionation in tropical and temperate grassland soils. *Funct. Ecol.* 14, 108–114. <https://doi.org/10.1046/j.1365-2435.2000.00402.x>.
- Savarese, C., Drosos, M., Spaccini, R., Cozzolino, V., Piccolo, A., 2021. Molecular characterization of soil organic matter and its extractable humic fraction from long-term field experiments under different cropping systems. *Geoderma* 383, 114700. <https://doi.org/10.1016/j.geoderma.2020.114700>.
- Schellekens, J., Buurman, P., 2011. N-Alkane distributions as palaeoclimatic proxies in ombrotrophic peat: the role of decomposition and dominant vegetation. *Geoderma* 164, 112–121. <https://doi.org/10.1016/j.geoderma.2011.05.012>.
- Schellekens, J., Buurman, P., Kalbitz, K., Zomer, A.V., Vidal-Torrado, P., Cerli, C., Comans, R.N.J., 2017. Molecular features of humic acids and fulvic acids from contrasting environments. *Environ. Sci. Technol.* 51, 1330–1339. <https://doi.org/10.1021/acs.est.6b03925>.
- Schnitzer, M., Khan, S.U., 1972. *Humic Substances in the Environment*. Marcel Dekker Inc, New York, NY.
- Six, J., Feller, C., Deneq, K., Ogle, S.M., de Moraes, J.C., Albrecht, A., 2002. Soil organic matter, biota and aggregation in temperate and tropical soils – effects of no-tillage. *Agronomie* 22 (7-8), 755–775.
- Sollins, P., Kramer, M.G., Swanston, C., Lajtha, K., Filley, T., Aufdenkampe, A.K., Wagai, R., Bowden, R.D., 2009. Sequential density fractionation across soils of contrasting mineralogy: evidence for both microbial- and mineral-controlled soil organic matter stabilization. *Biogeochemistry* 96, 209–231. <https://doi.org/10.1007/s10533-009-9359-z>.
- Spaccini, R., Piccolo, A., 2020. Amendments with humified compost effectively sequester organic carbon in agricultural soils. *Land Degrad. Dev.* 31, 1206–1216. <https://doi.org/10.1002/ldr.3524>.
- Sparks, D., Page, A., Helmke, P., Loepfert, R.H., Soltanpour, P., Tabatabai, M., Johnston, C., Sumner, M.E., 1996. In: *Methods of Soil Analysis*, SSSA Book Series. Soil Science Society of America, American Society of Agronomy, Madison, WI, USA. <https://doi.org/10.2136/sssabookser5.3>.
- Stevenson, F.J., 1982. *Humus Chemistry: Genesis, Composition, Reactions*. John Wiley & Sons, New York, NY.
- Thevenot, M., Dignac, M.F., Rumpel, C., 2010. Fate of lignins in soils: a review. *Soil Biol. Biochem.* 42, 1200–1211. <https://doi.org/10.1016/j.soilbio.2010.03.017>.
- Tinoco, P., Almendros, G., González-Vila, F.J., 2002. Impact of the vegetation on the lignin pyrolytic signature of soil humic acids from Mediterranean soils. *J. Anal. Appl. Pyrol.* 64, 407–420. [https://doi.org/10.1016/S0165-2370\(02\)00041-4](https://doi.org/10.1016/S0165-2370(02)00041-4).
- Toosi, E.R., Clinton, P.W., Beare, M.H., Norton, D.A., 2012. Biodegradation of soluble organic matter as affected by land-use and soil depth. *Soil Sci. Soc. Am. J.* 76, 1667–1677. <https://doi.org/10.2136/sssaj2011.0437>.
- van der Hage, E.R.E., Mulder, M.M., Boon, J.J., 1993. Structural characterization of lignin polymers by temperature-resolved in-source pyrolysis—mass spectrometry and Curie-point pyrolysis—gas chromatography/mass spectrometry. *J. Anal. Appl. Pyrol.* 25, 149–183. [https://doi.org/10.1016/0165-2370\(93\)80038-2](https://doi.org/10.1016/0165-2370(93)80038-2).
- Vancampenhout, K., Schellekens, J., Slaets, J., Hatté, C., Buurman, P., 2016. Fossil redox-conditions influence organic matter composition in loess paleosols. *Quat. Int.* 418, 105–115. <https://doi.org/10.1016/j.quaint.2015.11.057>.
- Verstraeten, G., Vancampenhout, K., Desie, E., De Schrijver, A., Hlava, J., Schelfhout, S., Verheyen, K., Muys, B., 2018. Tree species effects are amplified by clay content in acidic soils. *Soil Biol. Biochem.* 121, 43–49. <https://doi.org/10.1016/j.soilbio.2018.02.021>.
- Vesterdal, L., Schmidt, I.K., Callesen, I., Nilsson, L.O., Gundersen, P., 2008. Carbon and nitrogen in forest floor and mineral soil under six common European tree species. *For. Ecol. Manage.* 255, 35–48. <https://doi.org/10.1016/j.foreco.2007.08.015>.
- Vesterdal, L., Clarke, N., Sigurdsson, B.D., Gundersen, P., 2013. Do tree species influence soil carbon stocks in temperate and boreal forests? *For. Ecol. Manage.* 309, 4–18. <https://doi.org/10.1016/j.foreco.2013.01.017>.
- Vitousek, P.M., Chadwick, O.A., 2013. Pedogenic thresholds and soil process domains in basalt-derived soils. *Ecosystems* 16, 1379–1395. <https://doi.org/10.1007/s10021-013-9690-z>.
- von Lütow, M., Kögel-Knabner, I., Ekschmitt, K., Flessa, H., Guggenberger, G., Matzner, E., Marschner, B., 2007. SOM fractionation methods: relevance to functional pools and to stabilization mechanisms. *Soil Biol. Biochem.* 39, 2183–2207. <https://doi.org/10.1016/j.soilbio.2007.03.007>.
- Wang, T., Camps-Arbestain, M., Hedley, C., 2016. Factors influencing the molecular composition of soil organic matter in New Zealand grasslands. *Agric. Ecosyst. Environ.* 232, 290–301. <https://doi.org/10.1016/j.agee.2016.08.016>.
- Wang, W., Lemaire, R., Bensakhria, A., Luat, D., 2022. Review on the catalytic effects of alkali and alkaline earth metals (AAEMs) including sodium, potassium, calcium and magnesium on the pyrolysis of lignocellulosic biomass and on the co-pyrolysis of coal with biomass. *J. Anal. Appl. Pyrol.* 163, 105479. <https://doi.org/10.1016/j.jaap.2022.105479>.
- Zegouagh, Y., Derenne, S., Dignac, M.F., Baruiou, E., Mariotti, A., Largeau, C., 2004. Demineralisation of a crop soil by mild hydrofluoric acid treatment: influence on organic matter composition and pyrolysis. *J. Anal. Appl. Pyrol.* 71, 119–135. [https://doi.org/10.1016/S0165-2370\(03\)00059-7](https://doi.org/10.1016/S0165-2370(03)00059-7).
- Zimmermann, M., Leifeld, J., Schmidt, M.W.I., Smith, P., Fuhrer, J., 2007. Measured soil organic matter fractions can be related to pools in the RothC model. *Eur. J. Soil Sci.* 58, 658–667. <https://doi.org/10.1111/j.1365-2389.2006.00855.x>.